Supplementary Information

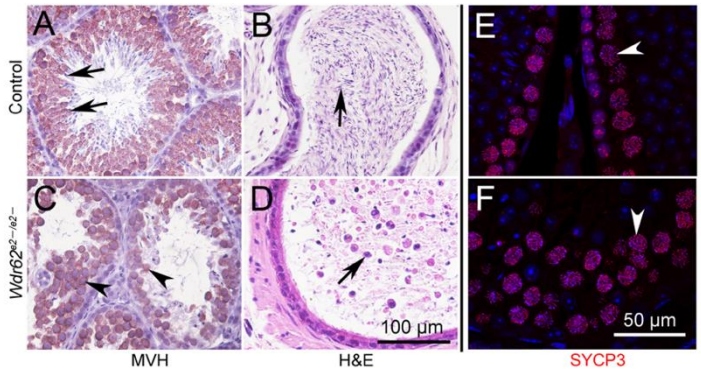

Fig. S1. Related to Fig. 1. Germ cells were arrested at the spermatocyte stage, and no mature sperm were observed in the epididymides of *Wdr62*-deficient mice. A large number of germ cells (C, black arrowheads) were observed in the seminiferous tubules of *Wdr62*$^{e2-/e2-}$ mice at 2 months of age, whereas no round/elongated spermatids were detected as in control testes (A, black arrows). The epididymides of control mice were filled with mature sperm (B, black arrows), whereas only cell debris was observed in *Wdr62*$^{e2-/e2-}$ mice (D, black arrows). A single layer of SYCP3-positive spermatocytes was observed in control testes (E, white arrowheads), whereas most of the germ cells in the seminiferous tubules of *Wdr62*$^{e2-/e2-}$ mice were SYCP3-positive (F, white arrowheads).

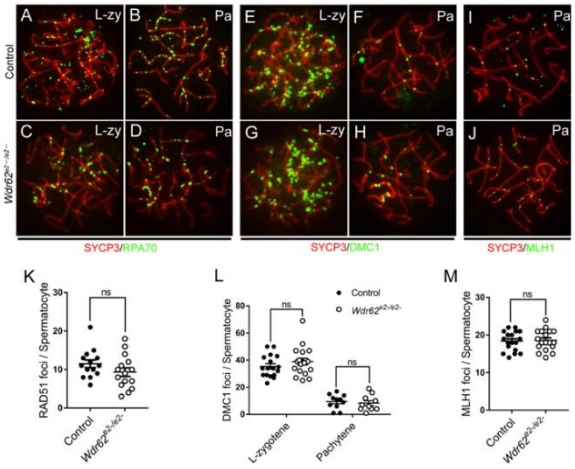

Fig. S2. Related to Fig. 2. No defect of DNA homologous recombination was observed in *Wdr62*-deficient germ cells. RPA70-positive foci (green) were detected on the chromosomes (red) of both control (A, B) and *Wdr62*-deficient (C, D) germ cells in the late zygotene (A, C) and pachytene (B, D) stages, and no difference was observed between control and *Wdr62*-deficient mice. A large number of DMC1-positive foci (green) were detected on the chromosomes (red) of both control (E, F) and *Wdr62*-deficient (G, H) germ cells in the late zygotene stage (E, G), and the number of foci (green) was dramatically reduced in the pachytene (F, H) stage in both control and *Wdr62*-deficient germ cells. Foci of the MLH1 protein (green) were observed in both control (I) and *Wdr62*$^{e2-/e2-}$ (J) germ cells at pachytene (I, J) stage. Quantification of the RAD51 foci per cell in control and *Wdr62*$^{e2-/e2-}$ mice at pachytene stage (K). Control (n=14), 11.5 ± 0.9931; *Wdr62*$^{e2-/e2-}$ (n=15) 9.333 ± 1.12. Quantification of the DMC1 foci per cell in control and *Wdr62*$^{e2-/e2-}$ mice at late-zygotene and pachytene stage (L). Late-zygotene: Control (n=17), 35.41±1.95; *Wdr62*$^{e2-/e2-}$ (n=18) 38.94 ± 2.526. Pachytene: Control (n=11), 9.455 ± 1.598; *Wdr62*$^{e2-/e2-}$ (n=10) 8.3 ± 1.844. Quantification of the MLH1 foci per cell in control and *Wdr62*$^{e2-/e2-}$ mice at pachytene stage (M). Control (n=18),18.39±0.6111; *Wdr62*$^{e2-/e2-}$ (n=18) 18.61±0.6424. The quantitative results were presented as the mean ± SEM from one experiment as the indicated number of cells. The significant difference was evaluated with *t*-test. P-value＞0.05 was considered as nonsense.

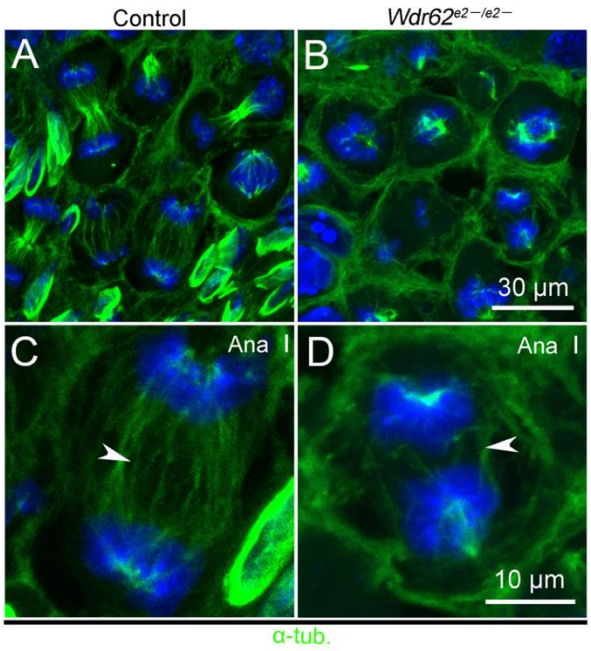

Fig. S3. Related to Fig. 4. Abnormal separation of chromosomes at anaphase I **in *Wdr62*-deficient germ cells**. In control mice, homologous chromosomes were separated at anaphase I with well-organized intermediate tubules (A, C, white arrowheads). Very few spermatocytes in anaphase I was observed in *Wdr62*$^{e2-/e2-}$ mice, and the intermediate tubules (B, D, white arrowheads) were seriously disrupted.

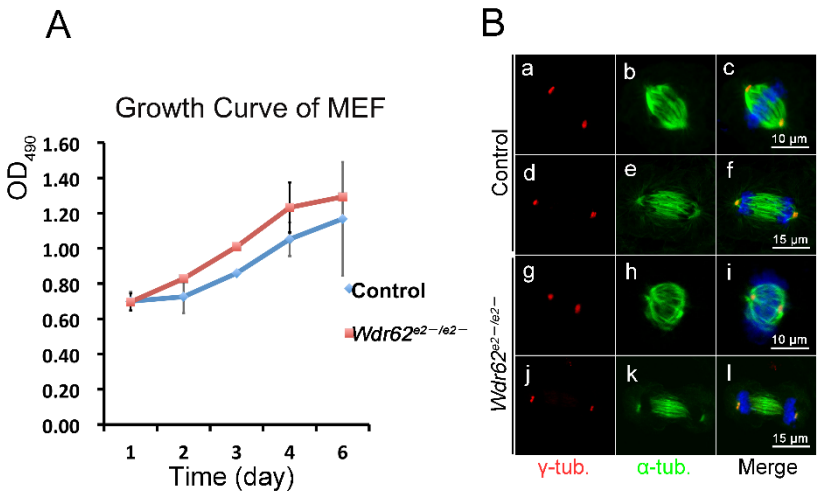

Fig. S4. Related to Fig. 5. The proliferation and spindle morphology of *Wdr62*-deficient MEF cells were not affected. MEF cells from control and *Wdr62*$^{e2-/e2-}$ mice were cultured *in vitro*, and the proliferation was examined by MTT assay. No difference in cell number and viability was observed between control and *Wdr62*-deficient MEF cells (A). The experiments were performed with three independent pools. The quantitative results were presented as the mean ± SEM. The significant difference was evaluated with *t*-test. P-value $>$ 0.05 was considered as nonsense. The morphology of the spindle and centrosome were examined by immunostaining (B). A well-organized spindle and a polar positioned centrosome in both control (a–f) and *Wdr62*-deficient (g–l) MEFs at metaphase (a–c, g–i) and anaphase (d–f, j–l) were observed.

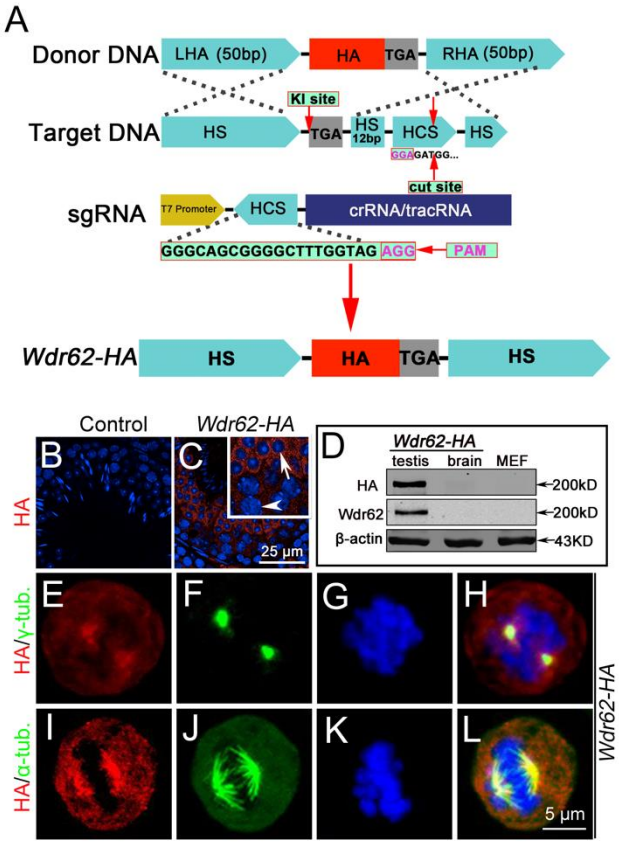

Fig. S5. Related to Fig. 6. WDR62 was abundantly expressed in spermatocytes/ spermatids and co-localized with the centrosome and spindle. (A) Schematic diagram for the generation of HA-tagged *Wdr62* knock-in mouse model using the CRISPR/Cas9 system. LHA/RHA, left/right homologous arms; HS, homologous sequences; HCS, homologous complementary sequence of gRNA; the protospacer-adjacent motif (PAM) sequence is labeled in pink; and the stop codon of *Wdr62* gene is labeled in the gray box. The results of immunofluorescence with anti-HA antibody showed *Wdr62* was highly expressed in spermatocytes (C, white arrowheads) and round spermatids (C, white arrows). WDR62 protein (~200 kD) was detected by western blot in the testes using both anti-HA and anti-WDR62 antibodies, but not in the brains and MEFs (D). WDR62 protein was localized in the cytoplasm of spermatocytes and co-localized with the centrosome (E–H) and spindle (I–L) at metaphase I.

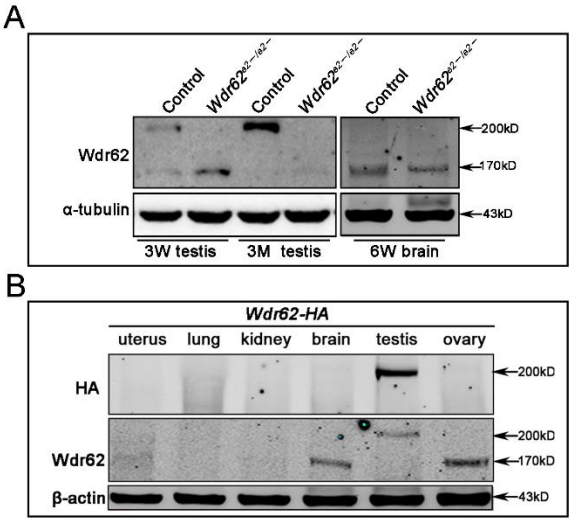

Fig. S6. Related to Fig. 6. The expression of different isoforms of the *Wdr62* gene in testes and other tissues. (A) A small (~170 kD) and a large (~200 kD) isoforms of protein were detected in the testes at 3 weeks by an anti-WDR62 antibody, but the large isoform was absent in *Wdr62*$^{e2-/e2-}$ testes. Only the large (~200 kD) isoform was detected in the testes at 3 months and was absent in *Wdr62*$^{e2-/e2-}$ testes. (B) The large isoform was only detected in adult testes by both anti-WDR62 and anti-HA antibodies. The small isoform was detected in the brain and ovary, but was not recognized by the anti-HA antibody.

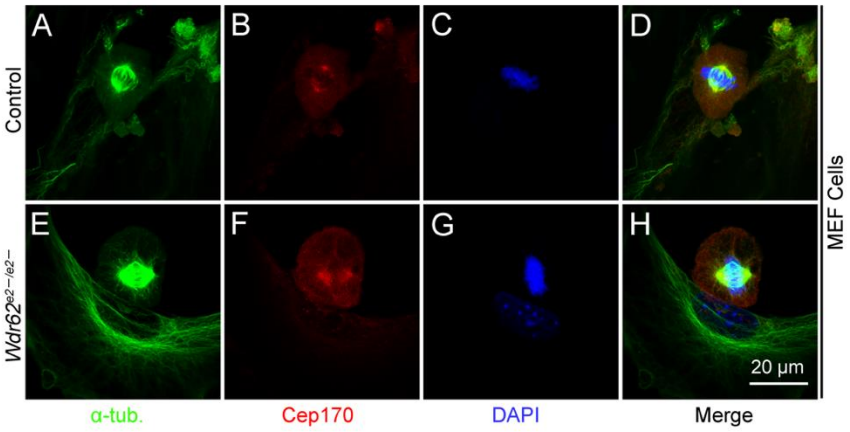

Fig. S7. Related to Fig. 6. The CEP170 positioning and spindle assembly of *Wdr62*-deficient MEF cells were not affected. A well-organized spindle and symmetrically located α-tubulin-positive spindles were observed in both control (A, D) and *Wdr62*-deficient (E, H) MEFs at metaphase (C, G). CEP170 protein was localized at the centrosome in control (B) and *Wdr62*-deficient (F) MEF cells.

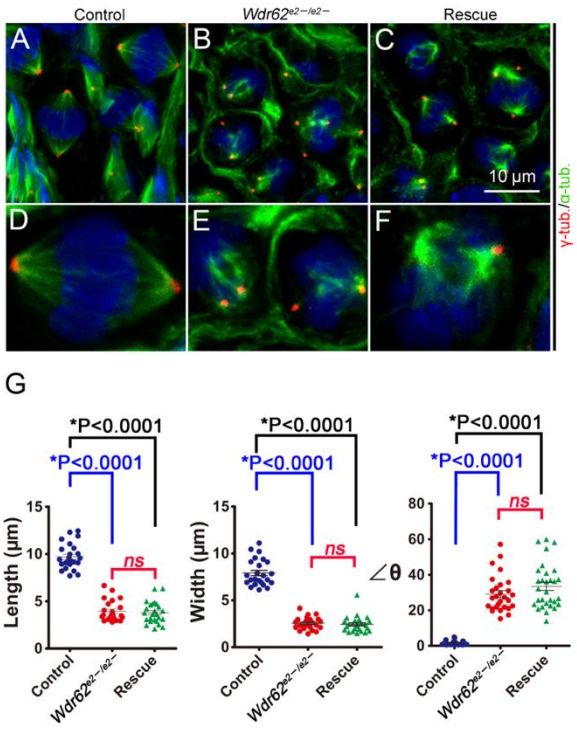

Fig. S8. Related to Fig. 8. The abnormality of spindle assembly in spermatocytes of *Wdr62*$^{e2-/e2-}$ mice was not rescued by JNK1 overexpression. Spindle and centrosome were labeled with anti-α-tubulin (green) and anti-γ-tubulin (red) antibodies. Compared with control (A, D), the polarity of the centrosome and structure of spindle were severely disrupted in *Wdr62*$^{e2-/e2-}$ mice (B, E), and this defect was not rescued in *Wdr62*$^{e2-/e2-}$*; CAJNK1*$^{+/flox}$*; Tnap-Cre* mice (Rescue) (C, F). (G) The quantitative analysis of the morphology of the spindle of spermatocytes at metaphase I in control, *Wdr62*$^{e2-/e2-}$, and Rescue mice. Count similar number of spermatocytes with α-tubulin-positive spindles in control, *Wdr62*$^{e2-/e2-}$ and Rescue testes, measure the parameters of spindles. Data are the mean ± SEM from one experiment with the indicated number of spermatocytes at Meta I (*p<0.0001) (Student's t-test).

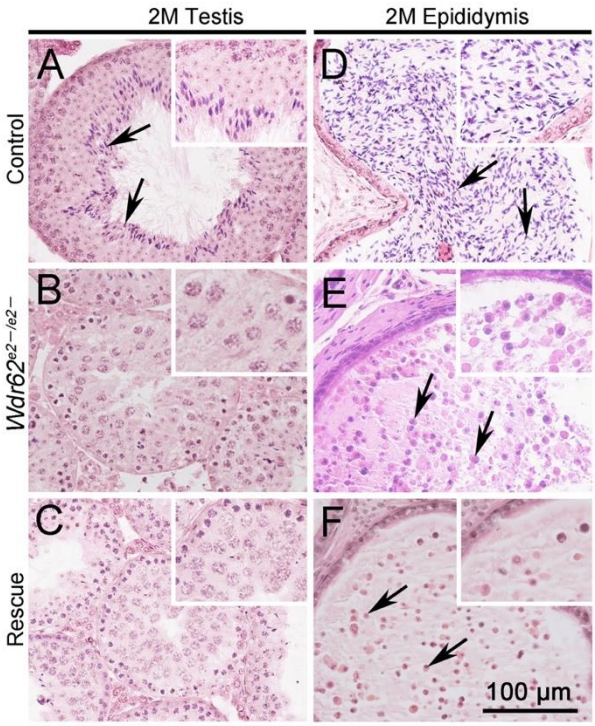

Fig. S9. Related to Fig. 8. The defect of spermatogenesis was not rescued in *Wdr62*$^{e2-/e2-}$; *CAJNK1*$^{+/flox}$; *Stra8-Cre* mice. Round and elongated spermatids were observed in control testes (A, black arrows), but only spermatocytes were observed in the seminiferous tubules of both *Wdr62*$^{e2-/e2-}$ (B, black arrowheads) and *Wdr62*$^{e2-/e2-}$; *CAJNK1*$^{+/flox}$; *Stra8-Cre* (C, black arrowheads) mice. Numerous mature sperm were observed in the epididymides of control mice (D, black arrows), but only cell debris was observed in the epididymides of *Wdr62*$^{e2-/e2-}$ (E, black arrows) and *Wdr62*$^{e2-/e2-}$; *CAJNK1*$^{+/flox}$; *Stra8-Cre* (F, black arrows) mice. Scale bars: 100 μm.

Supplementary Materials and methods

Mice

Wdr62$^{e2-/e2-}$ mice were obtained by crossing of *Wdr62*$^{+/e2-}$ mice. *Wdr62*$^{+/e2-}$ mice were generated as described previously (Zhou et al., 2018). The *Wdr62-HA* mouse lines were generated using CRISPR/Cas9 technology. *R26-JNKK2-JNK1 (JNK)* mice were acquired from Dr. Clive R Da Costa (Mammalian Genetics Laboratory, London Research Institute). *Wdr62*$^{e2-/e2-}$*;CAJNK1*$^{+/flox}$*;Tnap-Cre* mice and *Wdr62*$^{e2-/e2-}$*;CAJNK1*$^{+/flox}$*;Stra8-Cre* mice were generated by crossing *Wdr62*$^{+/e2-}$*;CAJNK1*$^{+/flox}$ mice with *Wdr62*$^{+/e2-}$*;Tnap-Cre* mice or *Wdr62*$^{+/e2-}$*;Stra8-Cre* mice. Genotyping (Gao et al., 2006; Higashino et al., 1999) was performed by PCR using DNA isolated from the tail tips of mice at 2 weeks. The tail tips were digested in 100 μL Solution A (25 mM NaOH + 0.2 mM EDTA) at 95℃ for 1 hour, followed with adding 100 μL Solution B (40 mM Tris-HCl).

Isolation of MEF cells

The embryos were dissected from control and mutant pregnant mice at E13.5 immediately after euthanasia, and washed in 1×PBS for three times. Then, transferred into serum-free medium and removed guts, head and limbs. The remaining bodies were dissected in 6 cm dishes with 1 ml DMEM and then digested by adding 3 ml 0.25% trypsin (Sigma) in a water bath with circular agitation (100 rpm) at 37°C for 15 min. The digestion was stopped by adding equal volume of 10% FBS. The MEF cell suspension was plated in 10 cm dishes with 10 ml DMEM (Invitrogen) supplemented with 10% FBS and 1% penicillin/streptomycin and cultured in a humidified 5% CO_2 at 37 ℃ (Gilks et al., 2004; Jian-Fu Chen, 2014).

Cell proliferation assay

MEF cells were cultured in DMEM of 96-well plates at 4×10^3 cells/well and counted at 1, 2, 3, 4, 5 or 6 days as described above. A volume of 20 μL 5 mg/mL MTT (Sigma) was added to each well and incubated at 37 ℃ for 4 hours. The corresponding product formazan were dissolved in 200 μL DMSO and the absorbance was measured by spectrophotometrically at 490 nm (OD_{490}) using a multifunction enzyme-linked analyzer.

CRISPR/Cas9

A 130-bp Wdr62-HA donor DNA was synthesized by Sangon Biotech (Shanghai). sgRNA was designed as Cas9-direct in Zhang Feng's laboratory online website (http://crispr.mit.edu/). The ~200-bp sgRNA fragment was amplified by PCR and transcribed with a MEGAshortscriptTM Kit (Ambion, AM1354). The Cas9 plasmid was linearized with Xba1 and transcribed with mMESSAGE mMACHINE® T7 Ultra Kit (Ambion, AM1345). RNA purification was performed with MEGAclear™ Kit (Ambion, AM1908). Cas9/gRNA/donor DNA co-injection of one-cell embryo was performed as previously described (Ma et al., 2014; Shen et al., 2013). Genotyping was performed by PCR as described previously using the DNA from tail biopsies.

Supplementary references

Gao, F., Maiti, S., Alam, N., Zhang, Z., Deng, J.M., Behringer, R.R., Lecureuil, C., Guillou, F., and Huff, V. (2006). The Wilms tumor gene, Wt1, is required for Sox9 expression and maintenance of tubular architecture in the developing testis. *Proc Natl Acad Sci U S A.* 103, 11987-11992.

Gilks, N., Kedersha, N., Ayodele, M., Shen, L., Stoecklin, G., Dember, L.M., and Anderson, P. (2004). Stress granule assembly is mediated by prion-like aggregation of TIA-1. *Mol Biol Cell.* 15, 5383-5398.

Higashino, M., Harada, N., Hataya, I., Nishimura, N., Kato, M., and Niikawa, N. (1999). Trizygotic pregnancy consisting of two fetuses and a complete hydatidiform mole with dispermic androgenesis. *Am J Med Genet.* 82, 67-69.

Jian-Fu Chen, L.N. (2014). Microcephaly Disease Gene Wdr62 Regulates Mitotic Progression of Embryonic Neural Stem Cells and Brain Size. *Nat Commun.*

Ma, Y., Zhang, X., Shen, B., Lu, Y., Chen, W., Ma, J., Bai, L., Huang, X., and Zhang, L. (2014). Generating rats with conditional alleles using CRISPR/Cas9. *Cell Res.* 24, 122-125.

Shen, B., Zhang, J., Wu, H., Wang, J., Ma, K., Li, Z., Zhang, X., Zhang, P., and Huang, X. (2013). Generation of gene-modified mice via Cas9/RNA-mediated gene targeting. *Cell Res.* 23, 720-723.

Zhou, Y., Qin, Y., Qin, Y., Xu, B., Guo, T., Ke, H., Chen, M., Zhang, L., Han, F., Li, Y., *et al.* (2018). Wdr62 is involved in meiotic initiation via activating JNK signaling and associated with POI in humans. *PLoS Genet.* 14, e1007463.